Jan 26, 2020

Modeling the Spread of 2019-nCoV

Collaborators This work is being led by Lauren Gardner at Johns Hopkins University CSSE, in collaboration with Aleksa Zlojutro and David Rey at rCITI at UNSW Sydney, and Ensheng Dong at JHU CSSE. Corresponding Email: l.gardner@jhu.edu

Modeling We implemented a previously published model that integrates both outbreak dynamics and outbreak control into a decision-support tool for mitigating infectious disease pandemics at the onset of an outbreak through border control. A stochastic metapopulation epidemic simulation tool is used to simulate global outbreak dynamics, and the border control mechanism considered is passenger screening upon arrival at airports (entry screening), which is used to identify infected or at-risk individuals. A detailed description of the model is provided at the end of this section.

Our metapopulation model is based on a global network of local, city-level, populations connected by edges representing passenger air travel between cities. At each node of the network, we locally model outbreak dynamics using a discrete-time Susceptible-Exposed-Infected-Recovered (SEIR) compartmental model. IATA monthly passenger travel volumes for all travel routes connecting airport pairs (including stopovers) is used to construct the weighted edges. The SEIR parameters are defined based on a 10 day period from exposure to recovery, aligning with a previously published report, divided into a 5 day incubation and 5 day recovery period for the purposes of this analysis. The effective contact rate corresponds to a reproductive number of 2, which aligns with an estimate from Imperial College London, reporting a range between 1.5 and 3.5. We assume initial cases of 2019-nCoV are only present in Wuhan, and no border control is accounted for. The model results presented are based on an average of 250 runs.

Results The simulation model is run for a time period between the start of the outbreak, up until January 25. The simulation results align with the number of air travel reported cases outside of mainland China early in the outbreak; specifically, we estimate 40 cases of 2019-nCoV to have been exported outside of mainland China by January 25, as was reported. For 40 cases to have been exported out of the country, we believe the number of 2019-nCoV cases in mainland China are likely much higher than that reported throughout January. Specifically, we estimate there to be around 20,000 cases of 2019-nCoV in mainland China on January 25 (at which time closer to 2000 were reported). We also estimate there were already hundreds of human cases of 2019-nCoV in Wuhan in early December. The estimated verses confirmed cases during January are presented in Figure 1. Our estimates are slightly higher than those from two other modeling exercises, namely, a report out of Imperial College estimated 4000 cases in mainland China on January 18, and a report out of Northeastern University estimated 12,700 on January 24.

However, there was a substantial and rapid increase in reported cases outside of China during these dates, which is still occurring, and likely to lead to higher estimates than those in this study.

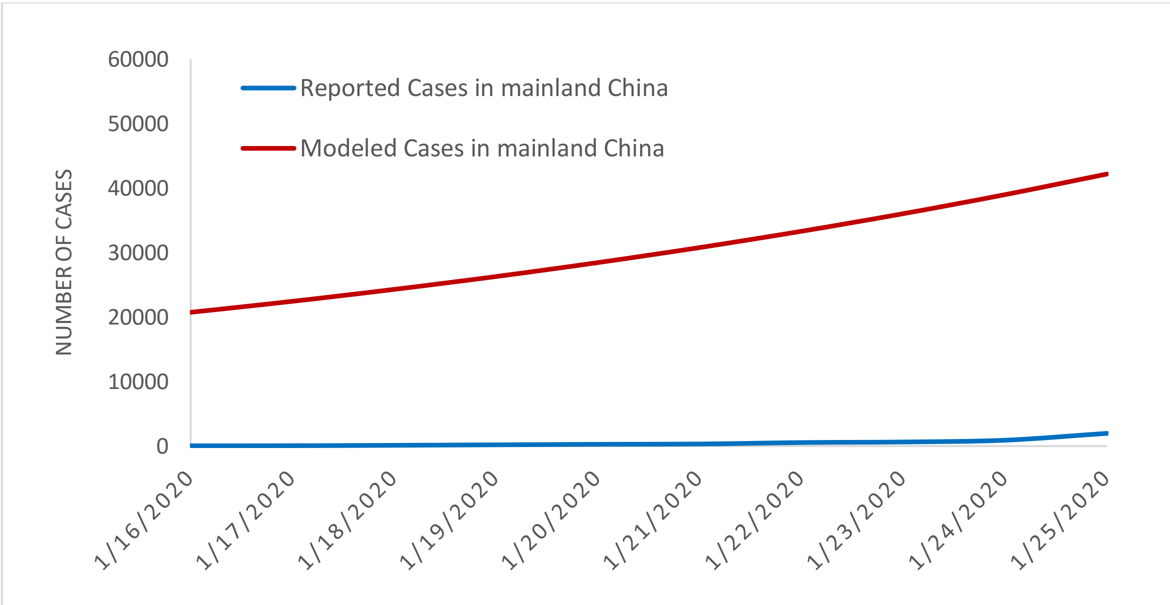

Figure 1 Estimated vs. Reported Cases of 2019 n-CoV cases globally

The simulation provides the expected number of imported cases arriving at each airport globally (based on final travel destinations of travelers) as of Jan 25. By aggregating this over all airports in a country we can estimate the total number of imported cases in each country. Figure 2 below illustrates our estimated number of imported cases arriving in each country compared with the number of 2019-nCoV reported cases as of January 26, at which time the 13 countries/regions we identify at highest risk have all reported at least one case.

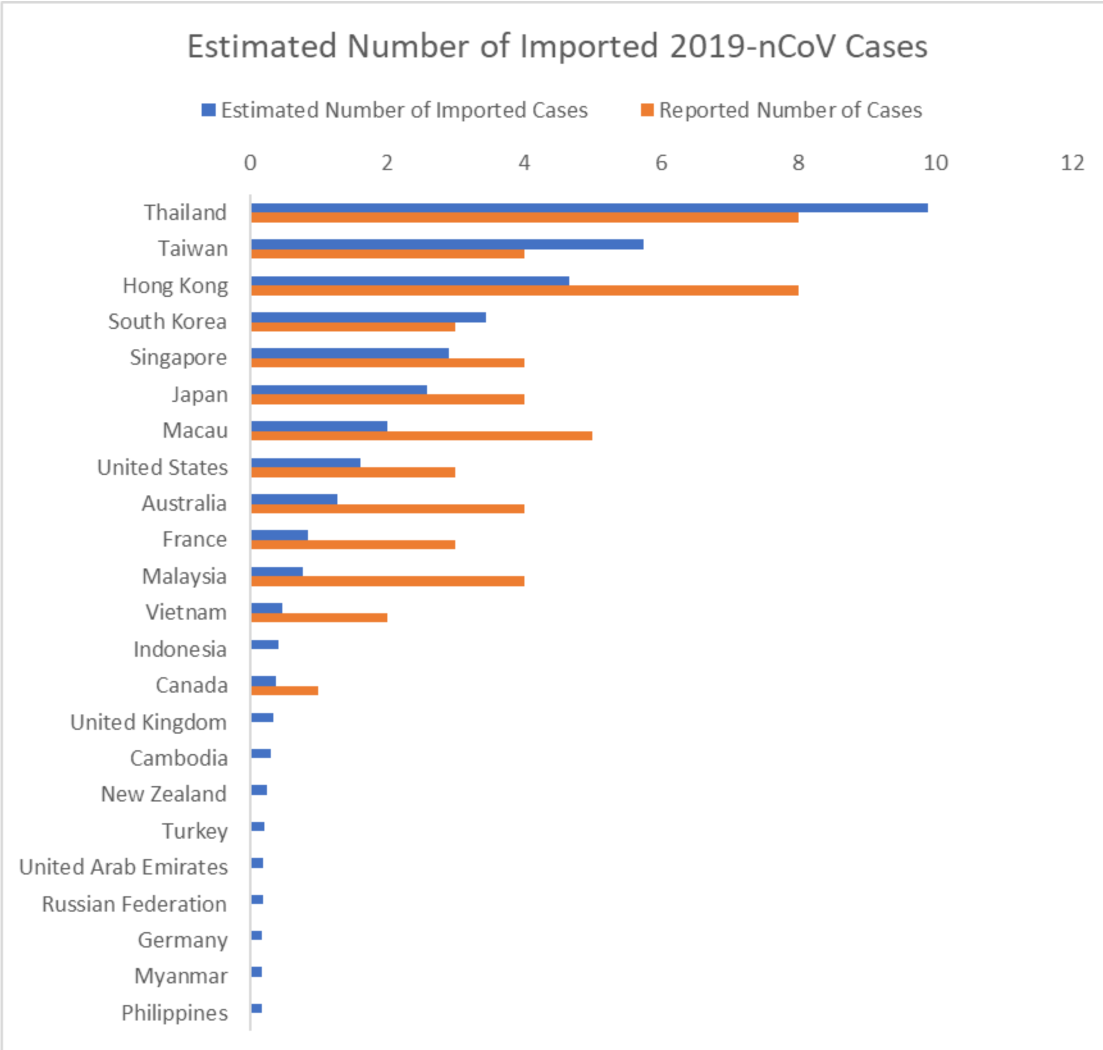

Figure 2. List of Countries/Regions with highest risk of imported 2019-nCoV cases

We further present the results at the airport level (based on their final travel destination), to identify the set of cities inside and outside mainland China at highest risk of case importation. The top 50 airports outside mainland China and within mainland China are illustrated in Figures 3 and 4, and listed in Table 1 and 2 below, respectively. The cities at highest risk are generally those in mainland China that receive high direct or indirect travel from WUH. While many of the cities outside mainland China that we identify at high risk have already reported cases, these cities should be prepared for additional cases to be reported over the coming days, likely in travelers whom departed Wuhan before the travel ban was implemented on January 23. In the U.S., our high risk airports have already been designated for screening by the CDC, namely LAX, JFK, SFO, ATL and ORD. By considering complete travel paths (with stopover airports), we identify additional airports that are at risk of exposure to infected travelers, and suggest the international airports in Seattle, Washington-Dulles, Newark, Detroit, Boston, Houston, Las Vegas, Dallas Fort Worth and Honolulu in the U.S., should also be considered for enhanced screening and security.

Figure 3. 50 Highest risk airports for 2019-nCoV arriving travelers outside mainland China.

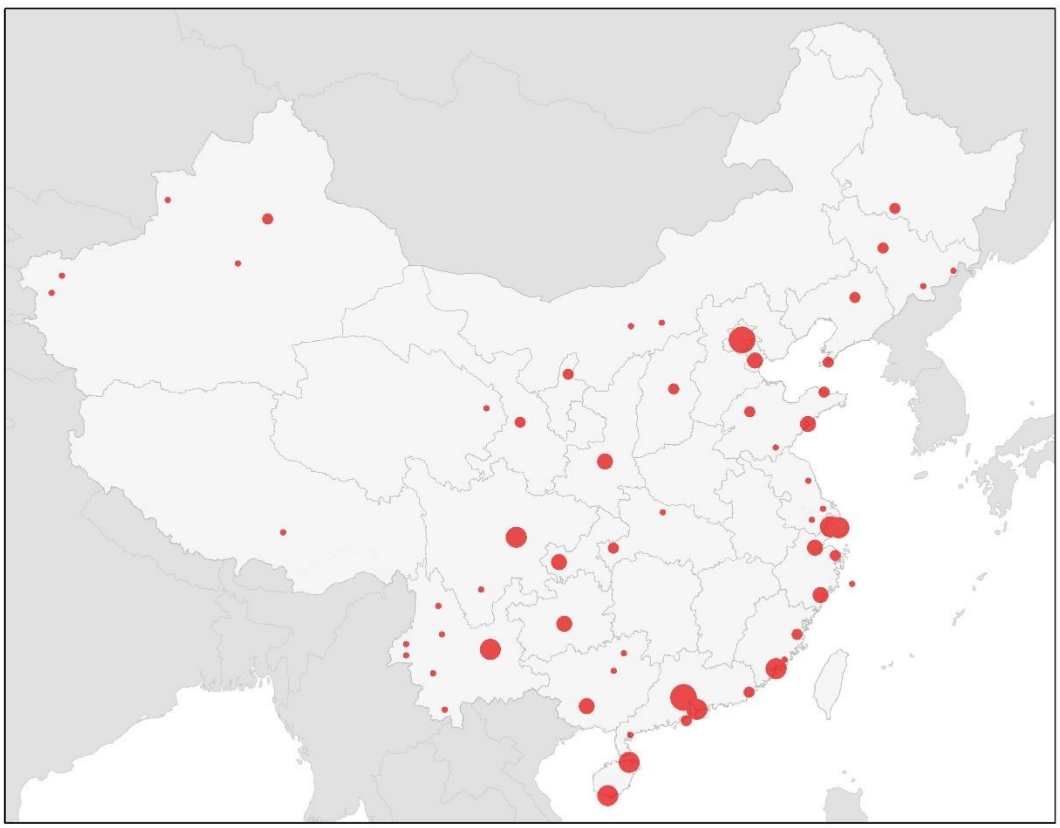

Figure 4. 50 Highest risk airports for 2019-nCoV arriving travelers in mainland China

Table 1. 50 Highest risk airports for 2019-nCoV arriving travelers outside mainland China.

Rank	Airport Code	Airport Name	City	Country/Region	Global Region
1	HKG	Hong Kong Intl	Hong Kong	Hong Kong	Asia
2	DMK	Don Muang International Airport	Bangkok	Thailand	Asia
3	BKK	Suvarnabhumi	Bangkok	Thailand	Asia
4	SIN	Changi	Singapore	Singapore	Asia
5	TPE	Taiwan Taoyuan International Airport	Taipei	Taiwan	Asia
6	ICN	Incheon International Airport	Seoul	South Korea	Asia
7	MFM	Macau International	Macau	Macau	Asia
8	KHH	Kaohsiung Intl	Kaohsiung	Taiwan	Asia
9	KIX	Kansai International	Osaka-Kansai	Japan	Asia
10	HKT	Phuket Intl	Phuket	Thailand	Asia
11	CJU	Jeju International	Jeju	South Korea	Asia
12	CDG	Charles De Gaulle	Paris-De Gaulle	France	Europe
13	KUL	Kuala Lumpur International Airport	Kuala Lumpur	Malaysia	Asia
14	TSA	Songshan	Taipei-Songshan	Taiwan	Asia
15	CNX	Chiang Mai Intl	Chiang Mai	Thailand	Asia
16	SFO	San Francisco Intl	San Francisco	United States	North America
17	TNN	Tainan	Tainan	Taiwan	Asia
18	LAX	Los Angeles Intl	Los Angeles	United States	North America
19	MEL	Melbourne Airport	Melbourne	Australia	Australasia
20	SYD	Kingsford Smith	Sydney	Australia	Australasia
21	SGN	Tan Son Nhat International Airport	Ho Chi Minh City	Vietnam	Asia
22	NRT	Narita	Tokyo-Narita	Japan	Asia
23	NGO	Chubu Centrair Intl	Nagoya	Japan	Asia
24	LHR	Heathrow	London-Heathrow	United Kingdom	Europe
25	FUK	Fukuoka	Fukuoka	Japan	Asia
26	KBV	Krabi Airport	Krabi	Thailand	Asia
27	CGK	Soekarno-Hatta Intl	Jakarta	Indonesia	Asia
28	IST	Ataturk	Istanbul	Turkey	Europe
29	JFK	John F Kennedy Intl	New York-JFK	United States	North America
30	YVR	Vancouver Intl	Vancouver	Canada	North America
31	AKL	Auckland Intl	Auckland	New Zealand	Australasia
32	DXB	Dubai International	Dubai	United Arab Emirates	Middle East
33	SVO	Sheremetyevo	Moscow-Sheremetyevo	Russian Federation	Europe
34	YYZ	Toronto Lester B. Pearson Intl	Toronto	Canada	North America
35	PNH	International	Phnom Penh	Cambodia	Asia
36	MNL	Ninoy Aquino Intl	Manila	Philippines	Asia
37	HND	Tokyo Intl (Haneda)	Tokyo-Haneda	Japan	Asia
38	RGN	Yangon International	Yangon	Myanmar	Asia
39	FSZ	Mount Fuji	Shizuoka	Japan	Asia
40	REP	Angkor International	Siem Reap	Cambodia	Asia
41	HDY	Hat Yai International	Hat Yai	Thailand	Asia
42	BNE	Brisbane Intl	Brisbane	Australia	Australasia
43	DPS	Ngurah Rai	Denpasar-Bali	Indonesia	Asia
44	KKC	Khon Kaen	Khon Kaen	Thailand	Asia
45	DEL	Indira Gandhi Intl	Delhi	India	Asia
46	FCO	Fiumicino	Rome-Da Vinci	Italy	Europe
47	FRA	Frankfurt International Airport	Frankfurt	Germany	Europe
48	NST	Nakhon Si Thammarat	Nakhon Si Thammarat	Thailand	Asia
49	URT	Surat Thani	Surat Thani	Thailand	Asia
50	MAD	Adolfo Suarez-Barajas	Madrid	Spain	Europe

Table 2. 50 Highest risk airports for 2019-nCoV arriving travelers in mainland China

Rank	Airport Code	Airport Name	City	Country/Region	Global Region
1	PEK	Capital International	Beijing	China	Asia
2	CAN	Baiyun International	Guangzhou	China	Asia
3	PVG	Pudong International	Shanghai	China	Asia
4	SHA	Hongqiao International	Shanghai-Metro	China	Asia
5	SZX	Bao'an International	Shenzhen	China	Asia
6	HAK	Meilan International	Haikou	China	Asia
7	SYX	Phoenix International	Sanya	China	Asia
8	KMG	Changshui International	Kunming	China	Asia
9	CTU	Shuangliu International	Chengdu	China	Asia
10	XMN	Gaoqi International	Xiamen	China	Asia
11	HGH	Xiaoshan International	Hangzhou	China	Asia
12	WNZ	Yongqiang International	Wenzhou	China	Asia
13	CKG	Jiangbei International	Chongqing	China	Asia
14	KWE	Longdongbao International	Guiyang	China	Asia
15	NNG	Wuxu International	Nanning	China	Asia
16	TSN	Binhai International	Tianjin	China	Asia
17	TAO	Liuting International	Qingdao	China	Asia
18	XIY	Xianyang International	Xi'an	China	Asia
19	SHE	Taoxian International	Shenyang	China	Asia
20	URC	Diwopu International	Urumqi	China	Asia
21	FOC	Changle International	Fuzhou	China	Asia
22	HRB	Taiping International	Harbin, P. R. China	China	Asia
23	ZUH	Sanzao International	Zhuhai	China	Asia
24	ENH	Xujiaping	Enshi	China	Asia
25	DLC	Zhoushuizi International	Dalian	China	Asia
26	NGB	Lishe International	Ningbo	China	Asia
27	INC	Hedong	Yinchuan	China	Asia
28	TYN	Wusu International	Taiyuan	China	Asia
29	SWA	Jieyang Chaoshan	Shantou	China	Asia
30	CGQ	Longjia International	Changchun	China	Asia
31	LHW	Zhongchuan	Lanzhou	China	Asia
32	YNT	Penglai International	Yantai	China	Asia
33	TNA	Yaoqiang International	Jinan	China	Asia
34	HET	Baita International	Hohhot	China	Asia
35	JJN	Jinjiang	Quanzhou	China	Asia
36	BAV	Erliban	Baotou	China	Asia
37	NTG	Xingdong	Nantong	China	Asia
38	LJG	Sanyi Airport	Lijiang	China	Asia
39	WUX	Sunan Shuofang	Wuxi	China	Asia
40	LZH	Bailian	Liuzhou	China	Asia
41	KWL	Liangjiang International	Guilin	China	Asia
42	HYN	Luqiao	Taizhou	China	Asia
43	XNN	Caojiabao	Xining	China	Asia
44	YNZ	Nanyang Airport	Yancheng	China	Asia
45	JHG	Xishuangbanna Gasa International	Jinghong	China	Asia
46	XFN	Liuji Airport	Xiangyang	China	Asia
47	NBS	Changbaishan	Baishan	China	Asia
48	LYI	Shubuling Airport	Linyi	China	Asia
49	KRL	Korla	Korla	China	Asia
50	ZHA	Zhanjiang	Zhanjiang	China	Asia

Limitations There are multiple modeling assumptions and limitations that should be noted regarding these estimates.

- In the day after this analysis was completed, travel reported cases increased by 40%, from 40 to 56. Therefore, it is likely the estimated number of cases reported in this study are a lower bound.
- There is still uncertainty about the transmission of 2019-nCoV, specifically surrounding the reproductive number and incubation period. The parameters chosen in this analysis fall in the uncertainty intervals provided to date. However, the substantial increase in cases being reported in late January indicate the parameters we used are too conservative, and the incubation period may be longer than we specified here, thus we are underestimating risk. More data will help us finer tune our estimates.
- Asymptomatic infections are not considered. If asymptomatic infections prove capable of spreading the virus, then these results would be further underestimating risk.
- The model only accounts for passenger air travel, and excludes mobility within and between cities via other modes of transport. Therefore, the spreading risk between regions connected via alternatives modes of travel is underestimated. This is most applicable to spread within China, which we are underestimating.
- The SEIR parameters used to model the outbreak within each city are deterministic. However, the spread of infected travelers moving between cities is modeled stochastically.
- Arrival passenger screening at airports and the complete air travel ban implemented in Wuhan on January 23 are not accounted for in this analysis. However, it is unlikely these policies impact the results presented, which are based on the start of the outbreak until January 26.
- No local control mechanisms (prophylaxtics, vaccines, school closures, quarantine efforts) within cities are accounted for. Thus, the R0 is assumed to be constant over time, and across all locations.
- We are using 2015 Travel data, because that is the most recent complete (airport-to-airport) data we had available in the lab.

Next Stages The next stage of our modeling exercise will be forward looking, with two main points of focus. First, will be the identification of those travel routes likely to continue spreading 2019-nCoV cases around the world, assuming travelers are no longer departing Wuhan directly. Second, we will identify the set of airports globally that should be prioritized for passenger screening.

Supplemental Model Description

Epidemic Simulation Model Our metapopulation model is based on a global air travel network which connects local, city-level, populations. Formally, the proposed metapopulation network can be represented by a graph $G = (V, E)$ where V is the set of nodes and E is the set of directed edges in the network. Nodes represent cities and edges represent passenger travel routes, possibly including stopovers, among cities. At each node of the network, we locally model outbreak dynamics using a discrete-time Susceptible-Exposed-Infected-Recovered (SEIR) compartmental model. The time steps are set to be $t \in T = \{1, 2, \ldots, t_{obs}\}$ where t_{obs} is the time step where the state of the outbreak is being evaluated. Local and global outbreak dynamics models are coupled by indexing compartmental states by network nodes $i \in V$ and time steps t. Specifically, we denote $S_{i,t}$, $E_{i,t}$, $I_{i,t}$ and $R_{i,t}$ the susceptible, exposed, infectious and recovered compartments at node i at time t. Because our focus is on the early stages of an outbreak (*e.g.*, weeks or months), we assume that nodes have time-independent populations and we denote N_i the population at node $i \in V$. We use this metapopulation model to capture day-to-day global travel dynamics, wherein the time steps are assumed to be of the order of magnitude of a day in length, which consistent with other studies that simulate infectious diseases dynamics at a global scale. Critically, the model incorporates a multi-commodity network flow model with time-dependent edge flows to model passenger movements from their origin node to their destination node. The path-based formulation, while more complex, enables more effective control decisions to be identified by the model. Specifically, the model is able to accurately capture the effect of controlling at stopover airports along a route, as well as identify the most cost-effective control decisions which utilize information about the entire path.

The governing infection dynamics of the SEIR model are used to model local outbreak dynamics in each city. For the purposes of this work the contact rate is assumed to be constant across populations. We denote β_i the (local) contact rate at node i, γ the transition or recovery rate and α the exposed parameter. In addition, we define $\lambda \in [0,1]$ the likelihood to travel when infectious, with $\lambda = 1$ representing the case where infected and healthy individuals are equally likely to travel. This parameter aims to represent the impact of reduced travel demand when infectious individuals are unable to travel due to severe symptoms. Unless otherwise noted, $\lambda = 1$. To model intercity flow, we assume that compartmental edge flows are proportional to tail node states, i.e. the number of travelers in a state is proportional to the number of individuals in this state at the origin node. For compartments S and R, compartmental edge flows are assumed deterministic and equal to their expected values. However, since the compartmental edge flows of exposed and infectious passengers may be considerably smaller than that of other compartments, we model $E_{ij,t}^{k}$ and $I_{ij,t}^{k}$ as discrete random variables. This stochastic allocation of infected individuals to destinations is critical when modeling the early stages of an outbreak, thus enforcing integer, compartmental edge flows and preventing the movement of fractional exposed or infectious individuals. This approach captures the critical and inherent uncertainty of the destination of the first infected travelers. For full details on the model see (*1*)

Travel Data The metapopulation network is constructed using global passenger air travel data from 2015 provided by the International Air Transport Association (IATA). The data provided from IATA includes monthly passenger travel volumes for all travel routes connecting airport pairs (including stopovers), representing nearly 83% of global traffic volumes. The final network used in this study contains the top 99% of the travelled routes provided, resulting in a network with approximately 500,000 routes, 2,908 cities, and 3,267 airports. The city populations served by each airport are based on the population densities provided by Oak Ridge National Laboratory's LandScan. The population size for each city was based on a 50km radius centered on each airport as was done previously, and computed using open source Geographic Information Systems software QGIS (https://qgis.org/). In some cases, multiple cities are serviced by more than one airport, for which the all assigned airport flows are mapped to the same population.

Border Control Decisions To integrate control decisions within the above stochastic metapopulation network we model passenger screening upon arrival at airports as a control variable, representative of the proportion of arriving passengers successfully screened at a given airport. We denote $x_{i,t} \in [0,1]$ the control rate at node i at time step t. Control decisions can then be incorporated in the proposed metapopulation epidemic model, thus capturing the combined effects of screening passengers at multiple nodes along their travel route. The complete model can be viewed as a control-driven stochastic metapopulation epidemic model wherein variables $x_{i,t}$ represent the level of control over time space in the network

1. Zlojutro, A, Rey, D and L **Gardner***. (2019) "Optimizing border control policies for global outbreak mitigation". *Scientific Reports* 9:2216. DOI **https://doi.org/10.1038/s41598-019-38665-w** (Open Source link) **https://rdcu.be/bniOs**